

# ELECTRON TRANSPORT FOR THE LCLS-II-HE LOW EMITTANCE INJECTOR\*

Y. Nosochkov<sup>†</sup>, C. Adolphsen, R. Coy, C. Mayes, T. Raubenheimer, M. Woodley,  
SLAC, Menlo Park, CA, USA

## Abstract

The Low Emittance Injector (LEI) is a recent addition to the LCLS-II High Energy (LCLS-II-HE) Project under design at SLAC National Accelerator Laboratory. It will provide a second beam source capable of producing a low emittance electron beam that increases the XFEL photon energy reach to 20 keV. The LEI will include an SRF electron gun, a buncher system, a 1.3 GHz cryomodule, and a beam transport system with a connection to the LCLS-II beamline and a stand-alone diagnostic line. The LEI transport beamlines and diagnostic are discussed.

## INTRODUCTION

The Low Emittance Injector (LEI) [1] is a recent addition to the LCLS-II High Energy (LCLS-II-HE) Project [2]. It will (1) improve the beam brightness to increase the XFEL photon energy reach to 20 keV and (2) provide a second injector for higher LCLS-II availability. The goal is to achieve the LEI transverse beam emittance of 0.1 mmrad at 100 MeV energy and 100 pC bunch charge. The LEI will include a state-of-the-art SRF electron gun, a buncher system, an 8-cavity 1.3 GHz cryomodule (CM00), and a beam transport system with a dogleg connection to the LCLS-II beamline and a stand-alone diagnostic line. The LEI will be installed in a separate tunnel parallel to the LCLS-II injector tunnel – see plan view in Fig. 1, where the LEI is at the top of the figure and the LCLS-II injector is at the bottom. The LEI beam can be either (1) delivered to the LCLS-II beamline for further transport to undulators or (2) sent into a straight-ahead diagnostic line for stand-alone operation.

This paper primarily describes the LEI beam transport and diagnostic systems downstream of the CM00 cryomodule. The aforementioned transport include: (1) a matching section downstream of the cryomodule, (2) an achromatic dogleg connection from the LEI to the LCLS-II beamline, and (3) a diagnostic line that supports measurements of bunch emittance, energy, charge, spatial profile, and beam halo and dark current. As a future upgrade, a horizontal RF deflecting cavity (TCAV) [3] and RF cavity BPMs are proposed to be added in the reserved spaces which will enable measurements of bunch length, slice energy spread, and vertical slice emittance. For a cost-effective design, the beamlines are made as compact as possible based on the existing magnets and devices or existing designs at SLAC. The location of the LEI connection to the LCLS-II is carefully selected; it does not require any modification to the existing LCLS-II beamline components,

and the LCLS-II beam can operate normally when the LEI is in stand-alone operation.

## LEI MAIN BEAMLINE

Figure 1 shows the layout of the LEI and LCLS-II injector tunnels and the beamline components. The initial design is based on 6-m distance between the LEI and LCLS-II injector lines, however there is a plan to increase the separation. The latter will not affect the present design except lengthening the dogleg.

The LEI main beamline transports the beam to the LCLS-II. It starts at the SRF gun followed by a buncher system, an 8-cavity 1.3 GHz cryomodule (CM00), an optics matching section, and a dogleg which connects the LEI to the LCLS-II injector beamline. The LEI and LCLS-II are merged in the free area of the LCLS-II Laser Heater (LH) where the LEI optics match is done using six downstream LH quadrupoles.

When the LEI beam is delivered to the LCLS-II, the beam from the LCLS-II injector must be turned off. Alternatively, the LEI beam can be directed to the LEI diagnostic line for beam measurements in stand-alone operation. In this case, the dogleg dipoles are turned off, and the beam from the LCLS-II injector can operate normally.

The matching section downstream of the CM00 consists of four quadrupoles. It accommodates vacuum components, a beam halo and dark current collimator, and reserves space for a future horizontal RF deflector. The four quadrupoles along with an upstream CM00 quadrupole are sufficient for match to the downstream dogleg optics including scenario where the incoming lattice functions are altered due to upstream errors or design updates. Steering correctors and BPMs are included for orbit correction.

The dogleg section creates a 35° horizontal angle to direct the LEI beam towards the LCLS-II beamline. The bending is performed by two pairs of 17.5° horizontal dipoles located at the beginning and end of the dogleg. The four dipoles and eight quadrupoles are positioned symmetrically relative to the dogleg center. Optics functions in the dogleg and the upstream matching section are shown in Fig. 2 calculated using MAD8 [4].

The dogleg is designed to cancel both linear and second order dispersion in order to suppress the chromatic emittance growth; the emittance preservation was confirmed in tracking simulations. The linear dispersion is cancelled using a double-bend achromat (DBA) cell at each end of the dogleg. The second order dispersion (see Fig. 2) is cancelled by constraining the horizontal phase advance between the DBA centers to  $2\pi$ . Quadrupoles are powered symmetrically, yielding symmetric beta functions, which were minimized. Each dogleg quadrupole has a BPM and a steering corrector next to it for orbit correction.

\* Work supported by the Department of Energy Contract DE-AC02-76SF00515.

<sup>†</sup> yuri@slac.stanford.edu

Content from this work may be used under the terms of the CC BY 4.0 licence (© 2022). Any distribution of this work must maintain attribution to the author(s), title of the work, publisher, and DOI

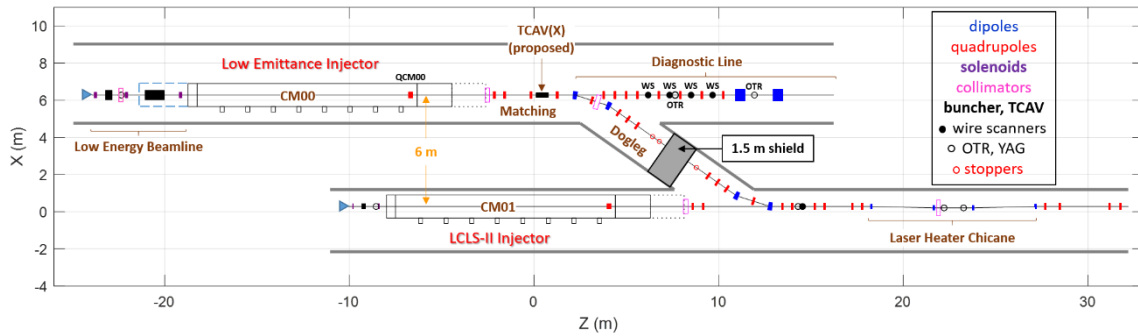


Figure 1: Plan view layout of the LEI and LCLS-II injector tunnels and beamlines.

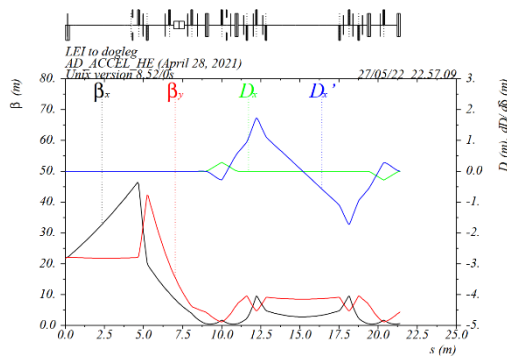


Figure 2: Beta functions and first and second order dispersion in the dogleg and the upstream matching section.

The dogleg  $R_{56}$  is 12.3 mm and  $T_{566}$  is 0.5 m. With the small bunch energy spread ( $<0.1\%$ ) in this region, these terms have negligible impact on the longitudinal phase space. The sufficiently large DBA dispersion allows energy collimation using an energy collimator near the center of the first DBA cell. The collimator adjustable aperture will be set for 3% of full-width energy acceptance in the dogleg. The design also reserves more than 4 m of free space at the dogleg center to accommodate a 1.5-m long radiation shield wall and three beam stoppers; they are required to allow occupancy in one injector tunnel while the other operates with beam.

Optics match from the LEI dogleg to the LCLS-II beamline is done using six LCLS-II Laser Heater quadrupoles downstream of the merge point. When the dogleg dipoles are off, the LH quadrupoles are set to their nominal LCLS-II strengths for beam operation from the LCLS-II injector. When the dogleg dipoles are turned on, the LEI beam is delivered to the LCLS-II, and the strengths of the six LH quadrupoles are set for a match with the LEI beam.

### LEI DIAGNOSTIC LINE

The LEI can operate in stand-alone mode by turning off the dogleg dipoles. In this case, the beam after the matching section proceeds straight-ahead into the LEI diagnostic section instead of being diverted towards the LCLS-II. Elevation view of the matching and diagnostic lines is shown in Fig. 3, where the first disabled dogleg dipole (BXDLI1) is depicted by a dashed box.

two  $\pm 35^\circ$  vertical dipoles lower the beam path by 1.4 m, directing it to 6-kW dump.

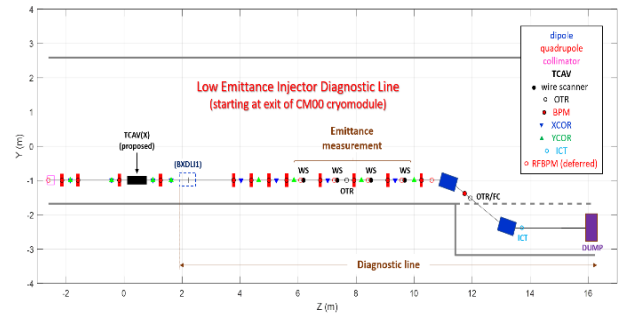


Figure 3: Elevation view of the diagnostic line and the upstream matching section.

The diagnostic line supports measurements of bunch emittance, energy, charge, spatial profile, and beam halo and dark current. The optics starts with four matching quadrupoles followed by two  $90^\circ$  FODO cells and two  $\pm 35^\circ$  vertical dipoles that form a dogleg. Each quadrupole has an associated steering corrector and BPM for orbit correction. The optics is matched to the same incoming lattice functions as in the LEI dogleg; it is shown in Fig. 4. Due to the use of existing type dipoles with special edge angles, the latter create an additional focusing as seen in Fig. 4.

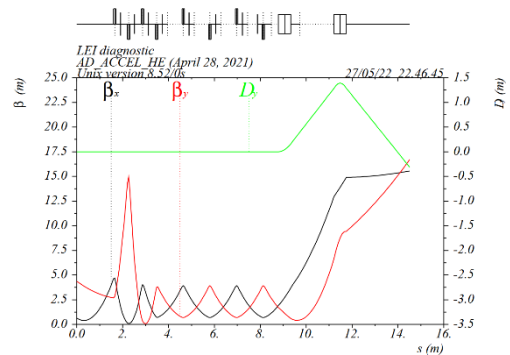


Figure 4: Lattice functions in the diagnostic line.

The two  $90^\circ$  FODO cells provide proper conditions for measurement of the projected transverse emittance using four fast wire scanners located at center of each half-cell [5]. Beam size at the wires is  $30 \mu\text{m}$  yielding 10% resolution with  $12.5 \mu\text{m}$  diameter Al:Si wires which have been in use in LCLS [6]. Lattice functions can be also measured

with the four wires. As a future upgrade, RF BPMs are proposed to be added upstream of each wire scanner to enable correction of beam position jitter during the measurements.

The first dipole at end of the diagnostic line serves as a spectrometer which allows high resolution energy spread measurements at the downstream OTR screen. The dipole creates large vertical dispersion (0.54 m) at the OTR where the vertical beta function is minimized, hence the measured vertical beam size is dominated by the dispersion and, therefore, correlates with the energy spread. A stripline BPM between the dipole and the OTR is used to assist with these measurements. In the future, it is proposed to replace this BPM with two RF-cavity BPMs placed on each side of the dipole to enable jitter correction during the measurements. The second diagnostic dipole cancels the vertical angle before the dump which significantly reduces the backscattered radiation from the dump into the LEI tunnel.

Beam charge in the spectrometer is measured using a Faraday Cup (FC), which is combined with the OTR in one custom-made device, and a Bergoz Integrating Current Transformer (ICT) included after the second diagnostic dipole (see Fig. 3).

A 2856 MHz horizontal RF deflecting cavity (TCAV) is proposed to be added to the LEI in the future that is similar to the one in the LCLS [3]. It will be located in the matching section as shown in Fig. 4. A horizontal kick from the TCAV will allow evaluation of the bunch length by measuring the horizontal beam size on the spectrometer OTR and the slice energy spread by measuring the vertical beam size. For these measurements, the quadrupole focusing will be adjusted to provide the optimal horizontal phase advance of  $\pi/2 \pmod{\pi}$  between the TCAV and the OTR. The latter will increase the phase advance in the two FODO cells with wires to  $114.9^\circ$ , which is less optimal for the emittance measurements on the wires. Hence, for an additional emittance measurement capability, a second OTR screen is included just after the second wire scanner (see Fig. 3). This will allow a separate measurement of the projected emittance using the technique of a quadrupole scan at this OTR [5, 7]. With the TCAV upgrade, the scan can be also used in combination with the TCAV kick for measurement of vertical slice emittance. For this measurement, the OTR location is optimized to provide closest to  $\pi/2 \pmod{\pi}$  horizontal phase advance from the future TCAV.

## MAGNETS AND DEVICES

For a cost-effective project, the LEI magnets, correctors and diagnostic devices are based on existing designs at SLAC. The magnet types are selected based on the required field strength and Beam Stay Clear (BSC) aperture. The BSC is consistent with the LCLS-II BSC definition using conservative assumptions of  $1 \mu\text{m}$  normalized emittance,  $\pm 2 \text{ mm}$  orbit errors,  $\pm 1\%$  energy jitter, and a core energy spread of  $\pm 0.5\%$  for the LEI beam delivered to the LCLS-II and  $\pm 1.9\%$  when using the diagnostic line.

Starting from the cryomodule, there are 21 LEI quadrupoles and 6 dipoles. The number of magnet power supplies is minimized taking advantage of the optics symmetry in the dogleg, two periodic FODO cells in the diagnostic line,

and identical strength dipoles in each of the dogleg and the diagnostic lines.

The LEI orbit correction system employs various types of steering correctors and BPMs. Five X/Y corrector pairs are distributed in the Low Energy Beamline (LEB) after the gun (see Fig. 1). One cold X/Y corrector package is included in each cryomodule (buncher and 8-cavity). Correctors and most BPMs in the matching, dogleg and diagnostic sections are placed next to quadrupoles to maximize their efficiency. The matching section X/Y correctors are arranged as a pair but powered independently. The dogleg and diagnostic line use separate X or Y correctors.

The LEI BPM system includes two stripline BPMs in the LEB, one cold button BPM per each cryomodule (buncher and 8-cavity), and 21 stripline BPMs in the downstream lines. The BPMs are part of the orbit correction system and can also measure bunch charge. Stripline BPM between the diagnostic spectrometer dipole and the downstream OTR is used to assist with energy spread measurements. This type BPM normally has two strips on the top and two strips on the bottom, thus providing large horizontal aperture. But due to the large vertical dispersion in the spectrometer this BPM is rotated by  $90^\circ$  to yield the required large vertical aperture. As a future upgrade, this BPM is proposed to be replaced with an RF cavity BPM. The upgrade plan also calls for an additional RF BPM upstream of the spectrometer dipole, an RF BPM at exit of the cryomodule, and four RF BPMs next to the four wire scanners. They will enable pulse-by-pulse jitter correction, and provide more accurate position, energy and bunch charge measurements.

The four diagnostic fast wire scanners can handle a beam rate of up to 0.6 MHz. They are placed periodically in two  $90^\circ$  FODO cells for measurement of projected emittance.

The LEI profile monitor system includes (1) two YAG profile monitors which are part of multi-function device containing also four collimators and a Faraday Cup in the LEB, (2) a diagnostic spectrometer OTR screen which is combined with a Faraday Cup in a custom-made device and used for energy spread measurements, and (3) an OTR near the second wire scanner for an alternate projected emittance measurement using quadrupole scans. The future TCAV upgrade will enable measurements of the bunch length and slice energy spread at the spectrometer OTR, and the vertical slice emittance at the other OTR.

The bunch charge monitors include one Bergoz ICT and a Faraday Cup in the LEB, the FC downstream of the spectrometer dipole, and the ICT before the diagnostic dump.

The LEI collimation system includes four interchangeable collimators with different fixed aperture in a multi-function device in the LEB which will collimate the beam halo and dark current from the gun. A fixed aperture beam halo and dark current collimator is included just after the CM00 cryomodule. Finally, an energy collimator is included in the first DBA cell of the dogleg where the beam size is dominated by horizontal dispersion.

A radiation protection shield wall and three beam stoppers will be installed near the center of the LEI dogleg (see Fig. 3). They are required to allow access to one injector tunnel while the other injector operates with beam.

## REFERENCES

- [1] "LCLS-II-HE low emittance injector conceptual design report," SLAC report LCLSIIHE-1.1-DR-0418-R0, Mar. 2022.
- [2] T. O. Raubenheimer, "The LCLS-II-HE, a high energy upgrade of the LCLS-II," in *Proc. FLS2018*, Shanghai, China, Mar. 2018, pp. 6-11. doi:10.18429/JACoW-FLS2018-MOP1WA02
- [3] R. Akre, L. Bentson, P. Emma, and P. Krejcik, "A transverse RF deflecting structure for bunch length and phase space diagnostics," in *Proc. PAC'01*, Chicago, USA, Jun. 2001, pp. 2353-2355.
- [4] H. Grote and F. C. Iselin, "The MAD program," <http://mad8.web.cern.ch/mad8/>.
- [5] M. G. Minty and F. Zimmermann, "Beam techniques – beam control and manipulation," SLAC-R-621, Apr. 2003.
- [6] B. Jacobson and P. Krejcik, private communication, Mar. 2021.
- [7] M. C. Ross, N. Phinney, G. Quickfall, H. Shoaee, and J. C. Sheppard, "Automated emittance measurements in the SLC," SLAC-PUB-4278, Mar. 1987.